

Quadratic diffusion Monte Carlo and pure estimators for atoms

A. Sarsa ¹, J. Boronat ², and J. Casulleras ²

¹ *International School for Advanced Studies, SISSA,*

Via Beirut 2/4, I-34014, Trieste, Italy

² *Departament de Física i Enginyeria Nuclear, Campus Nord B4-B5,
Universitat Politècnica de Catalunya, E-08034 Barcelona, Spain*

(October 29, 2018)

Abstract

The implementation and reliability of a quadratic diffusion Monte Carlo method for the study of ground-state properties of atoms are discussed. We show in the simple yet non-trivial calculation of the binding energy of the Li atom that the method presented is effectively second-order in the time step. The fulfilment of the expected quadratic behavior relies on some basic requirements of the trial wave function used for importance sampling, in the context of the fixed-node approximation. Expectation values of radial operators are calculated by means of a pure estimation based on the forward walking methodology. It is shown that accurate results without extrapolation errors can be obtained with a pure algorithm, explicitly reported, that can be easily implemented in any previous diffusion Monte Carlo program.

I. INTRODUCTION

Quantum Monte Carlo (QMC) methods have been widely employed in quantum chemistry calculations [1–4]. Nowadays, QMC methods have achieved accuracies comparable with CI calculations, mainly for small atoms and molecules. QMC is specially well suited to obtain the ground-state energy, providing an accurate treatment of electronic correlations in atomic and molecular systems. Apart from some technical and/or algorithmic differences, all the QMC methods pursue a common objective which is to solve the Schrödinger equation by relating the Green’s function of the system to a random walk. In the present work, we will focus on the diffusion Monte Carlo (DMC) method, based on a short time approximation to the Green’s function. The required antisymmetry of the atomic and molecular ground-state wave functions leads to the well-known sign problem. The present analysis is restricted to the standard fixed-node (FN) approximation [1,3]. According to the FN method, a prefixed nodal surface is defined in the configuration space of the system. That model nodal surface, which does not change along the calculation, introduces a boundary condition that forbids any crossing through a node. It has been proved that the resulting FN energy is an upper bound to the exact ground-state energy [3], the quality of the upper bound being related to the overlap between the model and the exact nodal surfaces.

The DMC method is simpler than domain Green’s function Monte Carlo [5] but, contrary to this, DMC presents a time-step Δt dependence that requires additional analysis. In general, the use of a finite Δt to approximate the imaginary-time Green’s function introduces a bias in the calculation. That problem is addressed by using several small time steps and then extrapolating the results for the energy to the $\Delta t \rightarrow 0$ limit. The simplest implementation of DMC uses a short-time Green’s function which is accurate to order $(\Delta t)^2$ (Eq. 5). In this case, one obtains energies that behave linearly with sufficiently small Δt and then an extrapolation to zero time-step is unavoidable. In order to reduce that large time-step dependence, and hence accelerate the rate of convergence of the calculation, several algorithms have been proposed [6–10]. Reynolds *et al.* [3,4] introduced an accept/reject step after the gaussian and drift movements in order to exactly sample $(\Phi_0)^2$ for all time steps if the exact wave function Φ_0 were used for importance sampling. Since in a true calculation the trial wave function is close to the exact one, the time-step dependence is significantly decreased with respect to the linear case. On the other hand, the rejection method introduces the problematic issue of persistent configurations [11,9], giving rise to a somehow unpredictable behaviour of the final Δt dependence of the energy.

A second alternative to reduce the time-step bias is to work out second-order algorithms by considering short-time Green’s function accurate to order $(\Delta t)^3$ (Eq. 6). Some time ago, Chin [8] developed second-order propagators and proved the quadratic efficiency of them in several model problems. That approach, here referred to as quadratic DMC (QDMC) method, has been profusely used in the microscopic study of quantum fluids, mainly ^4He [12] and ^3He [13]. In all these applications, QDMC has proved to be a real second-order algorithm and therefore the time-step bias is much more under control than in linear DMC algorithms. It is worth noticing that liquid ^3He is a fermion system, and the presence of a fixed nodal surface (FN approximation) has not broken down the expected second-order accuracy [13]. This feature contradicts some preliminary conclusions [9] that questioned a $(\Delta t)^2$ behavior when using nodal trial functions. Recently, Forbert and Chin [14] have

improved the time-step accuracy by developing a fourth-order algorithm that has manifested a fourth-order power law in a exigent calculation like the binding energy of liquid ${}^4\text{He}$.

The use of importance sampling (ψ) in the DMC solution of the Schrödinger equation makes walkers to be distributed according to the mixed probability distribution $\psi\Phi_0$, and not $(\Phi_0)^2$. Therefore, mixed estimators, which are the natural output in DMC, are only unbiased when the operators in question coincide with the Hamiltonian H or commute with it. In a first and very common approximation the bias of mixed estimators of, for instance, radial operators are dealt with an extrapolation method [5]. Within this procedure, a less biased estimation is obtained from a proper linear combination of variational and mixed estimators. The efficiency of that linear extrapolation is strongly related to the variational quality of ψ , and the results so obtained are still biased in a quantity difficult to assess [15,16]. It is possible, however, to eliminate the uncertainties present in the extrapolation method using really pure estimators.

The objective of obtaining pure estimators has been accomplished by using different techniques mainly bilinear sampling [17], path integral formalism [18,19] and forward walking [20,15,21,22,16,23]. Among them, several implementations of forward walking have been the most explored algorithms to achieve unbiased estimations of radial operators. Following Liu *et al.* [24], the necessary ingredient to correct the mixed estimator, i.e., the quotient $(\Phi_0(\mathbf{R})/\psi(\mathbf{R}))$, can be obtained from the asymptotic offspring of the \mathbf{R} walker. In some implementations of that forward walking procedure, tagging algorithms [20–22] have been devised in order to estimate the asymptotic number of descendants. The complexity of an efficient tagging algorithm, together with the large fluctuations observed in the asymptotic offspring, have impeded its widespread use among the DMC community. However, there is a simpler algorithm to sample pure estimators which does not require any tagging algorithmic structure and that can be very easily incorporated in any DMC code [16]. This method has been checked in model problems and has proved its accuracy in many calculations of quantum liquids properties.

In this work, we address the two above discussed aspects of the DMC method: the problem of the time-step dependence and the sampling of the exact distribution to extract pure estimators. We propose the use of a second-order DMC algorithm, that presents small time-step errors, and unbiased estimators to calculate exact values for non differential properties. As it is commented in the next section, the implementation of that algorithm can be done rather straightforwardly in any DMC code. The reliability of the method has been analyzed by studying the ground state of atomic lithium. This simple but not trivial system has been chosen since, on one hand, presents all the ingredients to test the performance of the method, and on the other, there are very accurate calculations [25–28] with which we can compare our results.

The rest of the paper is organized as follows. In Sec. II, the QDMC algorithm and the pure estimation methodology is presented. Sec III is devoted to present and discuss the results. Finally, the main conclusions of the present work are presented in Sec. IV.

II. METHOD

A. Quadratic Diffusion Monte Carlo

The DMC method solves the Schrödinger equation in imaginary time for the function $f(\mathbf{R}, t) = \psi(\mathbf{R})\Phi(\mathbf{R}, t)$,

$$-\frac{\partial f(\mathbf{R}, t)}{\partial t} = -\frac{1}{2} \nabla_{\mathbf{R}}^2 f(\mathbf{R}, t) + \frac{1}{2} \nabla_{\mathbf{R}}(\mathbf{F}(\mathbf{R})f(\mathbf{R}, t)) + (E_L(\mathbf{R}) - E) f(\mathbf{R}, t), \quad (1)$$

$\Phi(\mathbf{R}, t)$ being the wave function of the system and $\psi(\mathbf{R})$ a trial function used for importance sampling. Equation (1) is written in atomic units, which are the ones used throughout this work. In Eq. (1), $E_L = \psi(\mathbf{R})^{-1}H\psi(\mathbf{R})$ is the local energy and $\mathbf{F}(\mathbf{R}) = 2\psi(\mathbf{R})^{-1}\nabla_{\mathbf{R}}\psi(\mathbf{R})$; \mathbf{R} stands for a $3N$ -coordinate vector and E is an arbitrary energy shift.

The r.h.s. of Eq. (1) may be written as the action of three operators O_i acting on the wave function $f(\mathbf{R}, t)$,

$$-\frac{\partial f(\mathbf{R}, t)}{\partial t} = (O_1 + O_2 + O_3) f(\mathbf{R}, t) \equiv O f(\mathbf{R}, t) \quad (2)$$

The three terms O_i are interpreted by similarity with classical differential equations. The first one, O_1 , corresponds to a free diffusion with a diffusion coefficient $D = 1/2$; O_2 acts as a driving force due to an external potential, and finally O_3 looks like a birth/death term. In Monte Carlo, the Schrödinger equation (2) is best suited when it is written in an integral form by introducing the Green's function $G(\mathbf{R}', \mathbf{R}, \Delta t)$, which gives the transition probability from an initial state \mathbf{R} to a final one \mathbf{R}' in a time Δt ,

$$f(\mathbf{R}', t + \Delta t) = \int G(\mathbf{R}', \mathbf{R}, \Delta t) f(\mathbf{R}, t) d\mathbf{R}. \quad (3)$$

More explicitly, the Green's function is given in terms of the operator O by

$$G(\mathbf{R}', \mathbf{R}, \Delta t) = \langle \mathbf{R}' | \exp(-O\Delta t) | \mathbf{R} \rangle. \quad (4)$$

Most applications of the DMC method work with the simplest version of the short-time approximation,

$$\exp(-O\Delta t) = \exp(-O_3\Delta t) \exp(-O_2\Delta t) \exp(-O_1\Delta t) + \mathcal{O}((\Delta t)^2). \quad (5)$$

This expansion generates a linear time-step dependence that is reproduced in any calculation when the dependence of the energy on Δt is analyzed. A significantly better behavior is obtained by expanding the exponential of the operator O to higher orders in Δt . A good compromise between algorithmic complexity and efficiency is obtained by using a second-order expansion (QDMC). In this case, the Green's function $G(\mathbf{R}', \mathbf{R}, \Delta t)$ is approximated by

$$\begin{aligned} \exp(-O\Delta t) &= \exp\left(-O_3\frac{\Delta t}{2}\right) \exp\left(-O_2\frac{\Delta t}{2}\right) \exp(-O_1\Delta t) \\ &\times \exp\left(-O_2\frac{\Delta t}{2}\right) \exp\left(-O_3\frac{\Delta t}{2}\right) + \mathcal{O}((\Delta t)^3). \end{aligned} \quad (6)$$

This decomposition, which is the one we have used in our calculations, is not unique as pointed out by Rothstein *et al.* [7] and Chin [8]. Introducing the above expansion (6) in Eq. (3) the Schrödinger equation, written in integral form, becomes

$$f(\mathbf{R}', t + \Delta t) = \int \left[G_3 \left(\mathbf{R}', \mathbf{R}_1, \frac{\Delta t}{2} \right) G_2 \left(\mathbf{R}_1, \mathbf{R}_2, \frac{\Delta t}{2} \right) G_1 (\mathbf{R}_2, \mathbf{R}_3, \Delta t) \right. \\ \left. \times G_2 \left(\mathbf{R}_3, \mathbf{R}_4, \frac{\Delta t}{2} \right) G_3 \left(\mathbf{R}_4, \mathbf{R}, \frac{\Delta t}{2} \right) \right] f(\mathbf{R}, t) d\mathbf{R}_1 \dots d\mathbf{R}_4 d\mathbf{R} . \quad (7)$$

In Eq. (7), the total Green's function G is split into the product of individual Green's functions G_i , each one associated to the single operator O_i . G_1 is the Green's function corresponding to the free diffusion term (O_1), and thus it is the well-known solution for a noninteracting system,

$$G_1(\mathbf{R}', \mathbf{R}, t) = (4\pi Dt)^{-\frac{3N}{2}} \exp \left[-\frac{(\mathbf{R}' - \mathbf{R})^2}{4Dt} \right] . \quad (8)$$

In the MC simulation, the evolution given by G_1 corresponds to an isotropic gaussian movement of size proportional to \sqrt{Dt} . The Green's function G_2 describes the movement due to the drift force appearing in O_2 ; its form is given by [6]

$$G_2(\mathbf{R}', \mathbf{R}, t) = \delta(\mathbf{R}' - \mathbf{R}(t)), \quad \text{where} \begin{cases} \mathbf{R}(0) = \mathbf{R} \\ \frac{d\mathbf{R}(t)}{dt} = D \mathbf{F}(\mathbf{R}(t)), \end{cases} . \quad (9)$$

Under the action of G_2 , the walkers evolve in a deterministic way according to the drift force $\mathbf{F}(\mathbf{R}(t))$. In order to preserve the second-order accuracy in the time step, the differential equation (9) must also be solved with a second-order integration method. Finally, the third individual Green's function G_3 has an exponential form with an argument that depends on the difference between the local energy of a given walker and the prefixed value E ,

$$G_3(\mathbf{R}', \mathbf{R}, t) = \exp [-(E_L(\mathbf{R}) - E) t] \delta(\mathbf{R}' - \mathbf{R}). \quad (10)$$

This third term, which is called the branching factor, assigns a weight to each walker according to its local energy. Depending on the value of this weight the walker is replicated or eliminated in the population list. A pseudo code which describes the evolution of a walker for a time step Δt is presented in Ref. [29]. It is worth noticing that a second-order algorithm, like the one presented here, does not introduce any new terms with respect to a linear approximation. Therefore, it is quite simple to move from a linear code to a second-order one from the programmer's point of view.

As mentioned earlier, instead of using higher-order evolution operators some authors have been using a linear DMC method which incorporates an accept/reject step (Metropolis DMC -MDMC-) [3,4]. After a proposed gaussian plus drift movement for an individual electron, the new position is accepted with probability

$$p = \min \left(\frac{|\psi(\mathbf{R}')|^2 G(\mathbf{R}, \mathbf{R}', \Delta t)}{|\psi(\mathbf{R})|^2 G(\mathbf{R}', \mathbf{R}, \Delta t)}, 1 \right) . \quad (11)$$

The detailed balance condition (11) ensures theoretically a more accurate sampling of $|\psi|^2$, but introduces in DMC the potential problem of persistent configurations. Results obtained with the MDMC method show a significant reduction of the time-step bias, with respect to DMC, but its efficiency depends on the particular system under study and the extrapolation law to $\Delta t = 0$ can show erratic behaviors [30].

B. Pure Estimators

When the asymptotic limit ($t \rightarrow \infty$) is reached, the sampling of an operator O is carried out according to the mixed distribution $\psi\Phi_0$, with Φ_0 the ground-state wave function. Thus, the natural output in DMC corresponds to the so called *mixed* estimators. The mixed estimator of an operator $O(\mathbf{R})$ is, in general, biased by the trial wave function ψ used for importance sampling. Only when $O(\mathbf{R})$ is either the Hamiltonian, or commutes with it, the mixed estimation is the exact one. A simple method that has been widely used to approximately remove the bias present in the mixed estimations is the extrapolated estimator [5],

$$\langle O(\mathbf{R}) \rangle_e = 2 \langle O(\mathbf{R}) \rangle_m - \langle O(\mathbf{R}) \rangle_v , \quad (12)$$

from the knowledge of the mixed estimator $\langle O(\mathbf{R}) \rangle_m$ and the variational one

$$\langle O(\mathbf{R}) \rangle_v = \frac{\langle \psi(\mathbf{R}) | O(\mathbf{R}) | \psi(\mathbf{R}) \rangle}{\langle \psi(\mathbf{R}) | \psi(\mathbf{R}) \rangle} . \quad (13)$$

The expectation values obtained through the extrapolation method (12) depend on the trial wave function ψ used for importance sampling. Therefore, in spite of using good trial wave functions, the extrapolated estimator is always biased in a quantity difficult to assess a priori. In order to overcome that important restriction, one can go a step further and calculate *pure* (exact) expectation values,

$$\langle O(\mathbf{R}) \rangle_p = \frac{\langle \Phi_0(\mathbf{R}) | O(\mathbf{R}) | \Phi_0(\mathbf{R}) \rangle}{\langle \Phi_0(\mathbf{R}) | \Phi_0(\mathbf{R}) \rangle} . \quad (14)$$

Having in mind that walkers evolve according to the mixed distribution $\psi\Phi_0$, the pure estimator is more conveniently written as

$$\langle O(\mathbf{R}) \rangle_p = \left\langle \Phi_0(\mathbf{R}) \left| O(\mathbf{R}) \frac{\Phi_0(\mathbf{R})}{\psi(\mathbf{R})} \right| \psi(\mathbf{R}) \right\rangle / \left\langle \Phi_0(\mathbf{R}) \left| \frac{\Phi_0(\mathbf{R})}{\psi(\mathbf{R})} \right| \psi(\mathbf{R}) \right\rangle . \quad (15)$$

Some time ago, Liu *et al.* [24] proved that $\Phi_0(\mathbf{R})/\psi(\mathbf{R})$ can be obtained from the asymptotic offspring of the \mathbf{R} walker. Assigning to each walker \mathbf{R}_i a weight $W(\mathbf{R}_i)$ proportional to its number of future descendants

$$W(\mathbf{R}) = n(\mathbf{R}, t \rightarrow \infty) , \quad (16)$$

Eq. (15) becomes

$$\langle O(\mathbf{R}) \rangle_p = \frac{\sum_i O(\mathbf{R}_i) W(\mathbf{R}_i)}{\sum_i W(\mathbf{R}_i)} , \quad (17)$$

where the summatory \sum_i runs over all walkers and all times in the asymptotic regime. The difficulty of the method, known as forward walking, lies on the estimation of the weight $W(\mathbf{R})$ (16). The weight of a walker existing at time t is not known until a future time $t' \geq t + T$, T being a time interval long enough so that Eq. (16) could be replaced by $W(\mathbf{R}(t)) = n(\mathbf{R}(t'))$.

The evaluation of Eq. (17) has traditionally required the implementation of a tagging algorithm [20–22]. The purpose of that algorithm is to know, at any time during the simulation, which walker of any precedent configuration originated a present walker. In this way, one can determine the number of descendants of each \mathbf{R}_i , and accumulate its contribution to Eq. (17) from the distance. An easier method consists in working only with the present values of $O(\mathbf{R}_i)$, in such a way that a weight proportional to its future progeny is automatically introduced [16]. The schedule of this second algorithm is the following. The set of walkers at a given time $\{\mathbf{R}_i\}$, and the values that the operator O takes on them $\{O_i\}$, evolve after a time step to $\{\mathbf{R}'_i\}$ and $\{O'_i\}$, respectively. In the same time step, the number of walkers N changes to N' . In order to sample the pure estimator of O , we introduce an auxiliary variable $\{P_i\}$, associated to each walker, and that evolves with it (its final average value will provide the pure expectation value of O). The evolution law for $\{P_i\}$ is given by

$$\{P_i\} \rightarrow \{P'_i\} = \{P_i^t\} + \{O'_i\} , \quad (18)$$

where $\{P_i^t\}$ is the old set $\{P_i\}$ transported to the new one, in the sense that each element P_i is replicated as many times as the \mathbf{R}_i walker, without any other changes. $\{P_i\}$ is initialized to zero when the run starts.

In order to better fulfill the asymptotic condition (16) the evolution of the $\{P_i\}$ values is further carried on by means of

$$\{P_i\} \rightarrow \{P'_i\} = \{P_i^t\} . \quad (19)$$

Since a calculation is usually divided in blocks, one can collect/transport data during a block via Eq. (18), and allow for a only reweighting by means of Eq. (19) in the following one. Thus, after a first initialization block, each new block gives a value for the pure expectation value of O

$$\langle O(\mathbf{R}) \rangle_p = \sum_{i=1}^{N_f} \{P_i\} / (M \times N_f) , \quad (20)$$

M being the length of the block and N_f the number of walkers at the end of each reweighting block. A pseudo code for the pure estimation is available in Ref. [29]. It is worth mentioning that the algorithm can be easily generalized to DMC programs that work with branching weights.

The pure estimation depends on the size M of the block. M has to be large enough to match the asymptotic regime required by the forward walking property (16). With an easy modification of the code reported in Ref. [29], one can introduce a pure estimator for a set of increasing values of M in a single calculation. Looking at the results obtained, as a function of the block size, one observes a characteristic value M_c from which on the pure estimator is the same (considering the respective statistical errors).

III. RESULTS

The efficiency and accuracy of both the QDMC method and the pure estimator described in the previous section are analyzed in a calculation of ground-state properties of atomic Li. This is a well-known system, with nearly exact results, and serves well to our purpose since it contains the ingredients that can hinder the pursued second-order behavior: a nodal surface and cusp conditions. The present calculation works in the fixed-node approximation and therefore the energy obtained is an upper-bound to the ground-state energy of the atom. The trial wave function used for the importance sampling is the usual Jastrow-Slater form

$$\psi = \psi_J \phi^\uparrow \phi^\downarrow, \quad (21)$$

with ϕ^\uparrow (ϕ^\downarrow) the Slater determinant of spin up (spin down) electrons. The two-body Jastrow factor is taken as

$$\psi_J = \prod_{i < j} \exp\left(\frac{C_{ij} r_{ij}}{1 + b r_{ij}}\right), \quad (22)$$

with coefficients $C_{ij} = 1/2$ ($C_{ij} = 1/4$) for spin-unlike (spin-like) electrons to satisfy the electron-electron cusp conditions.

The functional forms for the orbitals entering in ϕ are taken from Ref. [23],

$$\begin{aligned} \chi^{1s} &= e^{-\zeta_{1s} r} e^{-wr/(1+vr)} \\ \chi^{2s} &= (1 + cr) e^{-\zeta_{2s} r} e^{-wr/(1+vr)}. \end{aligned} \quad (23)$$

They introduce an additional exponential, with respect to hydrogenic-like orbitals, to better fit the electron-nuclear correlations. The fulfilment of the electron-nuclear cusp condition introduces two constraints that reduce the number of parameters to be variationally optimized to four: b , v , ζ_{1s} , and ζ_{2s} . We have taken for them the values reported by Langfelder *et al.* [23].

The VMC energy obtained with ψ is in agreement with the one reported in Ref. [23], $E = -7.4737(1)$. That supposes a 90% of the correlation energy, which is significantly high taking into account the relatively simple trial wave function used. That result coincides with the more sophisticated wave function ψ_7 proposed by Schmidt and Moskowitz [31], and is slightly worse than the energy obtained using ψ_{17} ($E = -7.47669$) from the same authors. In a DMC calculation, like the one intended here, the proposal of Langfelder *et al.* [23] is more appropriate since it satisfies both the electron-electron and electron-nuclear cusp conditions. These requirements are essential in order to eliminate divergences of the drift force that break down the expected time-step accuracy. In fact, we have verified that if ψ_7 is used instead of ψ a second-order behavior is not achieved.

One of the main concerns of the present work is the time-step dependence of the different DMC algorithms discussed in Sec. II. In Table I, results for the energy as a function of Δt are reported using linear DMC, linear DMC with rejection (MDMC) and second-order DMC (QDMC). The *exact* non relativistic ground state energy is -7.478 060 323 10(31), calculated variationally by using a multiple basis set in Hylleraas coordinates [26]. The last row in Table I contains the extrapolation to $\Delta t = 0$ based on a polynomial fit to the data. The QDMC results follow the expected second-order behavior

$$E(\Delta t) = E_0 + E_2 (\Delta t)^2 \quad (24)$$

with good accuracy ($\chi^2/\nu = 1.2$). The extrapolated energy $E_0 = -7.47805(2)$, which reproduces the exact value, is statistically indistinguishable from the energy obtained with $\Delta t = 0.003$. In fact, one may move in a range $\Delta t = 0.0025 - 0.0035$ without significant changes in the energy. This is a very useful feature which derives from the second-order Green's function used in the QDMC method, and that has been also observed in quantum liquids calculations [12,13].

The extrapolations corresponding to the DMC and MDMC calculations have been carried out with a second-degree polynomial that, differently from the QDMC case (24), includes a linear term. The variance of the DMC result is larger than the QDMC one and the energy obtained is slightly above the QDMC and exact energies. The different dependence on Δt of the DMC and QDMC algorithms is illustrated in Fig. 1a: DMC energies are essentially linear while QDMC ones are quadratic.

The introduction of an accept/reject step in the imaginary-time evolution modifies completely the time-step dependence of the DMC method. As is clear from Table I and Fig. 1b the MDMC method allows for a significant reduction of the time-step bias, mainly for large Δt . For values $\Delta t \geq 0.01$, the MDMC energies are closer to the exact result than the QDMC ones. However, when Δt is reduced the behavior of the energy shows a quite erratic behavior (see Fig. 1c) that makes difficult the extrapolation to zero time-step. The extrapolated value reported in Table I comes from a second-order polynomial fit. The value obtained, $-7.47810(14)$ is in agreement with the QDMC result but its variance is an order of magnitude larger.

The pure estimator described in Sec. II, in conjunction with the QDMC method, has been used to calculate expectation values of several radial operators. In particular, we have considered the first radial moments of both the one-body density and the two-body intracule and extracule densities [32], defined as

$$\begin{aligned} \langle r^n \rangle &= \frac{\langle \Psi | \sum_{i=1}^N r_i^n | \Psi \rangle}{\langle \Psi | \Psi \rangle} \\ \langle r_{ij}^n \rangle &= \frac{\langle \Psi | \sum_{i < j=1}^N r_{ij}^n | \Psi \rangle}{\langle \Psi | \Psi \rangle} \\ \langle R^n \rangle &= \frac{\langle \Psi | \sum_{i < j=1}^N R^n | \Psi \rangle}{\langle \Psi | \Psi \rangle} . \end{aligned} \quad (25)$$

In Eqs. (25), \mathbf{r}_i is the position vector of the i -electron, $\mathbf{r}_{ij} = \mathbf{r}_i - \mathbf{r}_j$, and $\mathbf{R} = (\mathbf{r}_i + \mathbf{r}_j)/2$ is the center of mass vector of electrons i and j . Those observables play an important role in the description of the structure and dynamics of atoms and molecules [32,33]. They have been calculated within different theoretical frameworks [25–28,32–44] to determine electronic properties, to interpret the Hund rules, to elucidate electron correlation effects, or to study elastic and inelastic form factors.

In Fig 2, we show the dependence of the pure expectation values of $\langle r \rangle$, $\langle r_{12} \rangle$, and $\langle R \rangle$ upon the number of time steps M of a block. In these calculations, more CPU time has been

invested for the largest values of the block length M in order to reduce the statistical noise. Nevertheless, the pure estimators reach very soon the asymptotic regime, for M values as low as $M \simeq 500$. The statistical error of the pure estimators, evaluated in the asymptotic regime, is typically less than twice the statistical error of the mixed estimators for a fixed CPU time. The asymptotic results, i.e., the *real* pure estimators, reproduce accurately the exact values. As a matter of comparison, the mixed estimations and the variational ones are also shown. With the mixed and variational estimators, one easily obtains the extrapolated values (12) that are also plotted in Fig. 2. In all cases, the extrapolated estimator does not match the exact values, manifesting a bias that depends on the particular operator. The above features are also applicable to the second-degree radial operators $\langle r^2 \rangle$, $\langle r_{12}^2 \rangle$, and $\langle R^2 \rangle$ which appear reported in Fig. 3.

Our best pure estimates for the $\langle r^n \rangle$, $\langle r_{12}^n \rangle$, and $\langle R^n \rangle$ moments are contained in Tables II, III, and IV, respectively. Within the statistical errors, all the pure results are in agreement with the values considered as exact. With nearly the same variance than the extrapolated values, pure estimators eliminate the bias which comes from the trial wave function. On the other hand, extrapolated values retain some bias from ψ which is certainly difficult to assert a priori. It is worthwhile determining the accuracy of pure estimators using different propagators like DMC or MDMC. For that purpose, we have also implemented the pure estimator algorithm to the MDMC program. The results obtained are reported in Tables II-IV. The pure MDMC results improve the extrapolated values but do not share the excellent quality obtained with the QDMC algorithm. Somehow, the reason for that is the use of effective time-steps in the branching factor, the accuracy of which is a crucial point to ensure the success of the method.

IV. CONCLUSIONS

In the present work, the time-step dependence of the diffusion Monte Carlo method and the implementation of pure estimators, both in atomic systems, have been addressed. The study has been carried out for Li since it already contains the necessary ingredients to test the method and, additionally, a lot of nearly exact data are available. Using a short-time Green's function accurate to $\mathcal{O}(\Delta t)^3$, we have proved that it is possible in atomic systems to have a quadratic behavior in the simulated energy as was reported in quantum-liquid calculations. To the best of our knowledge it is the first stringent test of QDMC on atomic systems with nodal surface. The accuracy obtained had been occasionally questioned due to the presence of the divergences that appear in the drift force near the nodes. The present results show that the presence of nodes is not a real handicap, a conclusion that coincides with the one achieved in a recent QDMC calculation of homogeneous (fermion) liquid ${}^3\text{He}$ [13]. The most crucial point to guarantee a success of the QDMC method is the correct fulfilment of the electron-electron and electron-nuclear cusps conditions. The energies obtained with the relatively simple model for ψ , proposed by Langfelder *et al.* [23], follow accurately the expected second-order behavior. Additional checks performed using better trial wave functions, from the variational view, but not satisfying the electron-nuclear cusp show a more erratic behavior of the function $E(\Delta t)$.

The second aim of the work has been the consideration of a rather simple pure estimator, based on the forward walking methodology. Pure results for different radial moments are in

agreement with exact values and are manifestly superior to the extrapolated estimations.

As a concluding remark, we think that the combination of a QDMC method and the pure estimation here presented constitutes an appropriate tool for studying atoms and small molecules. Moreover, and very importantly from the programmer's viewpoint, the effort *i)* moving from a usual DMC to QDMC, and *ii)* introducing a pure estimator, is really small.

ACKNOWLEDGMENTS

This research has been partially supported by DGESIC (Spain) Grant N^o PB98-0922, and DGR (Catalunya) Grant N^o 1999SGR-00146. A.S. acknowledges the Italian MURST for financial support.

REFERENCES

- [1] J. B. Anderson, J. Chem. Phys. **63**, 1499 (1975); J. Chem. Phys. **65**, 411 (1976).
- [2] D. M. Arnow, M. H. Kalos, M. A. Lee, and K. E. Schmidt, J. Chem. Phys. **77**, 3547 (1982).
- [3] P. J. Reynolds, D. M. Ceperley, B. J. Alder, and W. A. Lester Jr., J. Chem. Phys. **77**, 5593 (1982).
- [4] B. L. Hammond, W. A. Lester Jr., and P. J. Reynolds, *Monte Carlo Methods in ab initio Quantum Chemistry* (World Scientific, Singapore, 1994).
- [5] D. M. Ceperley and M. H. Kalos, in *Monte Carlo Methods in Statistical Physics*, edited by K. Binder (Springer, Berlin, 1979).
- [6] J. Vrbik and S. M. Rothstein, J. Comput. Phys. **63**, 130 (1986).
- [7] S. M. Rothstein, J. Vrbik, and N. Patil, J. Comput. Chem. **8**, 412 (1987).
- [8] S. A. Chin, Phys. Rev. A **42**, 6991 (1990).
- [9] C. J. Umrigar, M. P. Nightingale, and K. J. Runge, J. Chem. Phys. **99**, 2865 (1993).
- [10] M. Mella, G. Morosi, and D. Bressanini, Phys. Rev. E **61**, 2050 (2000).
- [11] H. Bueckert, S. M. Rothstein, and J. Vrbik, Canad. J. Chem. **70**, 366 (1992).
- [12] J. Boronat and J. Casulleras, Phys. Rev. B **49**, 8920 (1994).
- [13] J. Casulleras and J. Boronat, Phys. Rev. Lett. **84**, 3121 (2000).
- [14] H. A. Forbert and S. A. Chin, Phys. Rev. B **63**, 144518 (2001).
- [15] A. L. L. East, S. M. Rothstein, and J. Vrbik, J. Chem. Phys. **89**, 4880 (1988).
- [16] J. Casulleras and J. Boronat, Phys. Rev. B **52**, 3654 (1995).
- [17] S. Zhang and M. H. Kalos, J. Stat. Phys. **70**, 515 (1993).
- [18] S. Baroni and S. Moroni, Phys. Rev. Lett. **82**, 4745 (1999).
- [19] A. Sarsa, K. E. Schmidt, and W. R. Magro, J. Chem. Phys. **113**, 1366 (2000).
- [20] P. J. Reynolds, R. N. Barnett, B. L. Hammond, and W. A. Lester, Jr., J. Stat. Phys. **43**, 1017 (1986).
- [21] R. N. Barnett, P. J. Reynolds, and W. A. Lester, Jr., J. Comput. Phys. **96**, 258 (1991).
- [22] K. J. Runge, Phys. Rev. B **45**, 7229 (1992).
- [23] P. Langfelder, S. M. Rothstein, and J. Vrbik, J. Chem. Phys. **107**, 8525 (1997).
- [24] K. S. Liu, M. H. Kalos, and G. V. Chester, Phys. Rev. A **10**, 303 (1974).
- [25] F. W. King, Phys. Rev. A **40**, 1735 (1989).
- [26] Z. C. Yan and G. W. F. Drake, Phys. Rev. A **52**, 3711 (1995).
- [27] F. W. King, J. Chem. Phys. **102**, 8053 (1995).
- [28] F. J. Gálvez, E. Buendía, and A. Sarsa, Phys. Rev. A **61**, 052505 (2000).
- [29] See EPAPS Document No. for pseudo codes of the QDMC algorithm and pure estimators. This document may be retrieved via the EPAPS homepage (<http://www.aip.org/pubservs/epaps.html>) or from <ftp.aip.org> in the directory `/epaps/`. See the EPAPS homepage for more information.
- [30] H. A. Forbert, Ph. D. thesis, Texas A&M University, 1999.
- [31] K. E. Schmidt and J. W. Moskowitz, J. Chem. Phys. **93**, 4172 (1990).
- [32] A. J. Coleman, Int. J. Quantum Chem. **S1**, 427 (1967).
- [33] A. J. Thakkar, in *Density Matrices and Density Functionals*, edited by R. Erdahl and V. H. Smith Jr. (Reidel, Dordrecht, 1987).
- [34] R. O. Esquivel and A. V. Bunge, Int. J. Quantum. Chem. **32**, 295 (1987).
- [35] R. O. Esquivel, A. V. Bunge, and M. A. Nuñez, Phys. Rev. A, **43**, 3373 (1991).

- [36] R. N. Barnett, E. M. Johnson, and W. A. Lester, Jr., *Phys. Rev. A* **51**, 2049 (1995).
- [37] S. A. Alexander and R. L. Coldwell, *J. Chem. Phys.* **103**, 2572 (1995); **110** 10218 (1999).
- [38] H. Meyer, T. Müller, and A. Schweig, *J. Mol. Struct.: TEOCHEM* **360**, 55 (1996).
- [39] T. Koga and H. Matsuyama, *J. Chem. Phys.* **107**, 8510 (1997).
- [40] T. Koga and H. Matsuyama, *J. Chem. Phys.* **108**, 3424 (1998).
- [41] A. Sarsa, F.J. Gálvez, and E. Buendía, *J. Chem. Phys.* **109**, 7075 (1998).
- [42] F.J. Gálvez, E. Buendía, and A. Sarsa, *J. Chem. Phys.* **111**, 3319 (1999).
- [43] S. K. Worsnop, R. J. Boyd, J. M. Elorza, C. Sarasola, and J. M. Ugalde, *J. Chem. Phys.* **112**, 1113 (2000).
- [44] X. Fradera, M. Duran, and J. Mestres, *J. Chem. Phys.* **113**, 2530 (2000).
- [45] F. W. King and V. Shoup, *Phys. Rev. A* **33**, 2940 (1986).

TABLES

TABLE I. Energy of the Li atom versus the time step and using different algorithms. The figures enclosed in parenthesis are the statistical errors. The *exact* energy is $-7.4780632310(31)$

Δt	DMC	MDMC	QDMC
0.030	-7.45279(4)	-7.47860(4)	-7.48244(3)
0.0200	-7.46074(5)	-7.47844(3)	-7.48007(3)
0.0100	-7.46893(5)	-7.47831(4)	-7.47855(4)
0.0075	-7.47127(4)	-7.47810(3)	-7.47831(3)
0.0050	-7.47333(3)	-7.47811(3)	-7.47817(2)
0.0030	-7.47520(4)	-7.47827(4)	-7.47807(4)
extrapolation	-7.47784(11)	-7.47810(14)	-7.47805(2)

TABLE II. Estimations of $\langle r^n \rangle$ moments of the Li atom using the MDMC and QDMC algorithms.

	$\langle r \rangle$	$\langle r^2 \rangle$	$\langle r^3 \rangle$
Variational ^a	4.9553(7)	18.088(7)	91.12(6)
Extrapolated (MDMC)	4.992(3)	18.39(3)	92.8(3)
Extrapolated (QDMC)	5.001(3)	18.46(3)	93.3(3)
Pure (MDMC)	4.985(2)	18.32(2)	92.4(2)
Pure (QDMC) ^b	4.991(2)	18.36(2)	92.7(2)
<i>exact</i>	4.989523 ^c	18.354615 ^c	92.60364 ^d

^aVMC results of Ref. [23]: $\langle r \rangle = 4.9536(6)$, $\langle r^2 \rangle = 18.076(6)$

^bGSD-DMC results of Ref. [23]: $\langle r \rangle = 4.992(7)$, $\langle r^2 \rangle = 18.36(7)$

^cHylleraas expansion of Ref. [26]

^dHylleraas expansion of Ref. [25]

TABLE III. Estimations of $\langle r_{12}^n \rangle$ moments of the Li atom using the MDMC and QDMC algorithms.

	$\langle r_{12} \rangle$	$\langle r_{12}^2 \rangle$	$\langle r_{12}^3 \rangle$
Variational	8.593(2)	36.32(1)	189.2(1)
Extrapolated (MDMC)	8.673(7)	36.89(6)	192.4(5)
Extrapolated (QDMC)	8.686(7)	37.02(6)	193.5(5)
Pure (MDMC)	8.662(3)	36.79(3)	191.6(3)
Pure (QDMC)	8.671(3)	36.87(3)	192.4(3)
<i>exact</i>	8.668397 ^a	36.847838 ^a	192.10037 ^b

^aHylleraas expansion of Ref. [26]

^bHylleraas expansion of Ref. [45]

TABLE IV. Estimations of $\langle R^n \rangle$ moments of the Li atom using the MDMC and QDMC algorithms.

	$\langle R \rangle$	$\langle R^2 \rangle$	$\langle R^3 \rangle$
Variational	4.2615(7)	9.009(3)	23.48(2)
Extrapolated (MDMC)	4.301(3)	9.15(2)	23.9(4)
Extrapolated (QDMC)	4.309(4)	9.19(2)	24.05(7)
Pure (MDMC)	4.309(3)	9.19(2)	23.76(7)
Pure (QDMC)	4.300(2)	9.150(8)	23.89(4)
<i>exact</i>	4.2996(6) ^a	9.145(3) ^a	23.86(1) ^a

^aRef. [28]

FIGURES

FIG. 1. Total energy of the Li atom versus the time step Δt computed by using the DMC, MDMC and QDMC algorithms. The lines on top of the data correspond to polynomial fits: $E(\Delta t) = E_0 + E_1\Delta t + E_2(\Delta t)^2$ for DMC and MDMC, and $E(\Delta t) = E_0 + E_2(\Delta t)^2$ for QDMC. In all cases, the error bars are smaller than the size of the symbols. The dotted line stands for the exact energy. In a) the time-step dependence of the DMC and QDMC energies are compared. In b) the comparison is between QDMC and MDMC. Finally, c) illustrates the different behavior of MDMC and QDMC when $\Delta t \rightarrow 0$; notice the dispersion of the MDMC data compared with the regular behavior of the QDMC energies.

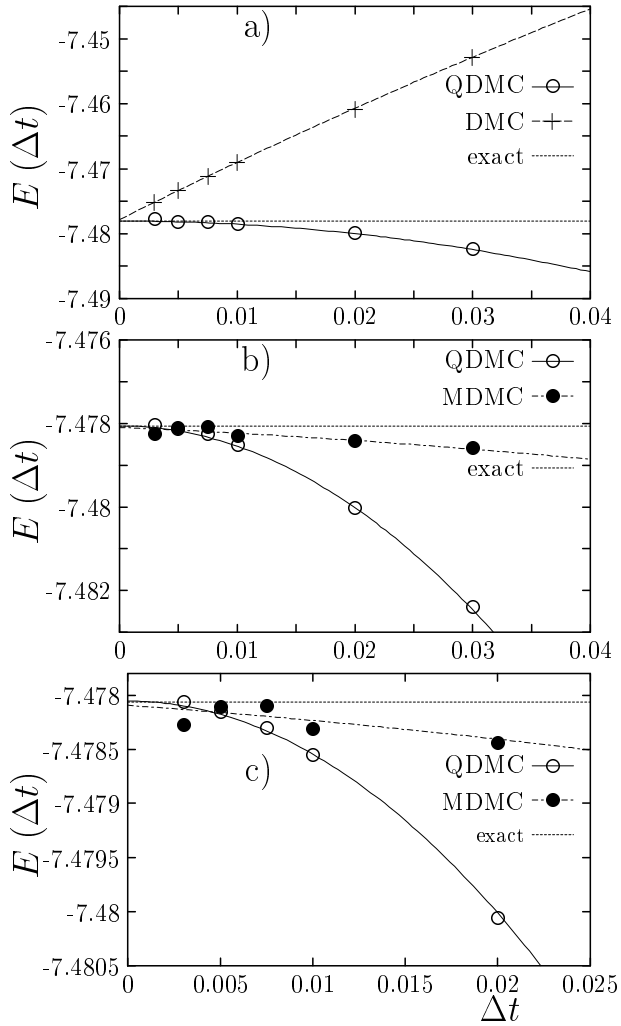


FIG. 2. Pure expectation values of first-degree radial moments of the Li atom as a function of the block length M . The solid, dashed, and dotted lines stand for the exact, variational, and extrapolated results, respectively.

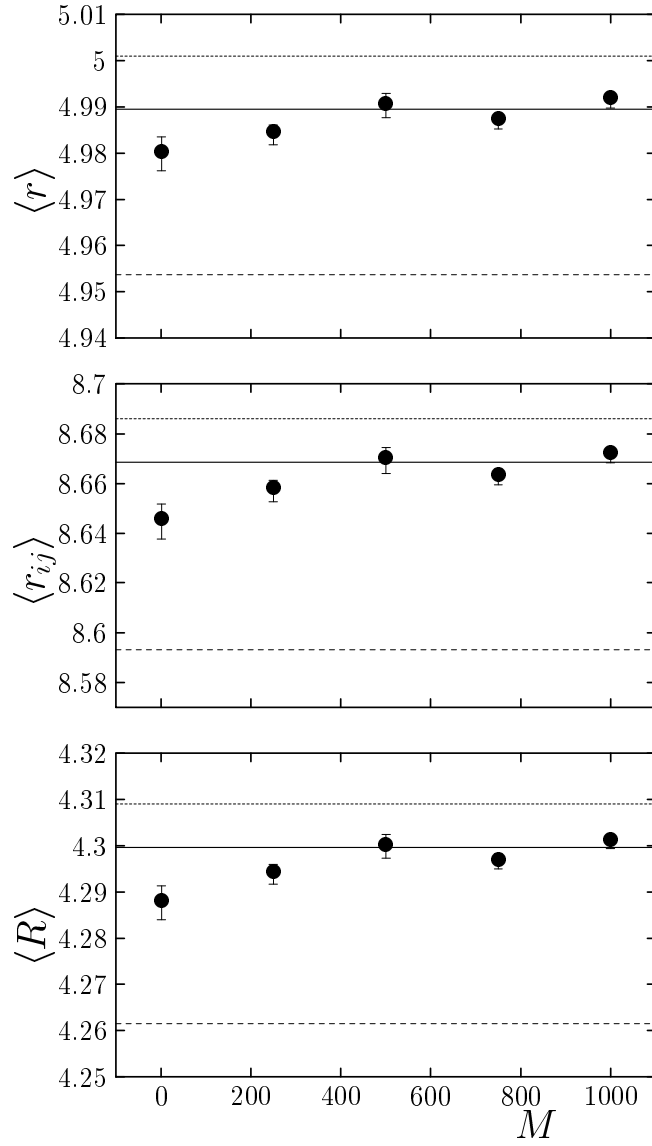


FIG. 3. Pure expectation values of second-degree radial moments of the Li atom as a function of the block length M . The solid, dashed, and dotted lines stand for the exact, variational, and extrapolated results, respectively.

